Coupling characteristics between two conical micro/nano fibers: simulation and experiment

Zehua Hong, Xinwan Li,* Linjie Zhou, Xiaowei Shen, Jianguo Shen, Shuguang Li and Jianping Chen

State Key Laboratory of Advanced Optical Communication Systems and Networks, Department of Electronic Engineering, Shanghai Jiao Tong University, Shanghai 200030, China
** lixinwan@sjtu.edu.cn*

Abstract: The coupling characteristics of conical micro/nano fibers (CMNFs) are investigated using numerical simulations and experiments. Distinct from uniform micro/nano fibers (UMNFs), the coupling efficiency not only depends on the overlapping length between two CMNFs but also the tapering angle of the CMNFs. With the increase of overlapping length, the coupling efficiency gradually converges to a stable value, with its convergence speed determined by the angle of the CMNFs. Experimental result shows the convergent coupling efficiency can be >90%. The spectral response of the coupler shows a "box-shape" profile with a 3-dB bandwidth of 2 nm, resembling a flat-top bandpass filter. And experimental results also show the coupling characteristics of CMNFs are overlapping length and taper angle dependent, which verify the simulation conclusions.

OCIS codes: (060.2340) Fiber optics components; (130.3990) Micro-optical devices; (230.4000) Microstructure fabrication.

References and links

1. L. Tong, R. R. Gattass, J. B. Ashcom1, S. He, J. Lou, M. Shen, I. Maxwell, and E. Mazur, "Subwavelength-diameter silica wires for low-loss optical wave guiding," Nature **426**(6968), 816–819 (2003).
2. L.-J. Chen, H.-W. Chen, T.-F. Kao, J. Y. Lu, and C. K. Sun, "Low-loss subwavelength plastic fiber for terahertz waveguiding," Opt. Lett. **31**(3), 308–310 (2006).
3. C.-Y. Chao, and L. Jay Guo, "Design and Optimization of Microring Resonators in Biochemical Sensing Applications," J. Lightwave Technol. **24**(3), 1395–1402 (2006).
4. F. Warken, E. Vetsch, D. Meschede, M. Sokolowski, and A. Rauschenbeutel, "Ultra-sensitive surface absorption spectroscopy using sub-wavelength diameter optical fibers," Opt. Express **15**(19), 11952–11958 (2007).
5. F. Xu, V. Pruneri, V. Finazzi, and G. Brambilla, "An embedded optical nanowire loop resonator refractometric sensor," Opt. Express **16**(2), 1062–1067 (2008).
6. D.-I. Yeom, E. C. Mägi, M. R. E. Lamont, M. A. Roelens, L. Fu, and B. J. Eggleton, "Low-threshold supercontinuum generation in highly nonlinear chalcogenide nanowires," Opt. Lett. **33**(7), 660–662 (2008).
7. D. Türke, S. Pricking, A. Husakou, J. Teipel, J. Herrmann, and H. Giessen, "Coherence of subsequent supercontinuum pulses generated in tapered fibers in the femtosecond regime," Opt. Express **15**(5), 2732–2741 (2007).
8. V. Grubsky, and A. Savchenko, "Glass micro-fibers for efficient third harmonic generation," Opt. Express **13**(18), 6798–6806 (2005).
9. Z. Zhang, X. Lu, Y. Zhang, M. Zhou, T. Xi, Z. Wang, and J. Zhang, "Enhancement of third-harmonic emission from femtosecond laser filament screened partially by a thin fiber," Opt. Lett. **35**(7), 974–976 (2010).
10. G. Brambilla, and F. Xu, "Adiabatic submicrometric tapers for optical tweezers," Electron. Lett. **43**(4), 204–206 (2007).
11. P. Pal, and W. H. Knox, "Fabrication and Characterization of Fused Microfiber Resonators," IEEE Photon. Technol. Lett. **21**(12), 766–768 (2009).
12. W. Yu, Z. Xu, H. Changlun, B. Jian, and Y. Guoguang, "A tunable all-fiber filter based on microfiber loop resonator," Appl. Phys. Lett. **86**(19), 191112 (2008).
13. M. Sumetsky, "Optical fiber microcoil resonators," Opt. Express **12**(10), 2303–2316 (2004).
14. M. Sumetsky, Y. Dulashko, J. M. Fini, and A. Hale, "Optical microfiber loop resonator," Appl. Phys. Lett. **86**(16), 161108 (2005).
15. D. Dai, and S. He, "Design of an ultrashort Si-nanowaveguide-based multimode interference coupler of arbitrary shape," Appl. Opt. **47**(1), 38–44 (2008).
16. X. Jiang, L. Tong, G. Vienne, X. Guo, A. Tsao, Q. Yang, and D. Yang, "Demonstration of optical microfiber knot resonators," Appl. Phys. Lett. **88**(22), 223501 (2006).

#138036 - $15.00 USD Received 11 Nov 2010; revised 9 Dec 2010; accepted 4 Jan 2011; published 14 Feb 2011

17. M. Sumetsky, Y. Dulashko, J. M. Fini, A. Hale, and D. J. DiGiovanni, "The Microfiber Loop Resonator: Theory,Experiment, and Application," J. Lightwave Technol. **24**(1), 242–250 (2006).
18. Y. Li, and L. Tong, "Mach-Zehnder interferometers assembled with optical microfibers or nanofibers," Opt. Lett. **33**(4), 303–305 (2008).
19. K. Huang, S. Yang, and L. Tong, "Modeling of evanescent coupling between two parallel optical nanowires," Appl. Opt. **46**(9), 1429–1434 (2007).
20. G. H. Wang, P. Shum, G. B. Ren, X. Yu, J. J. Hu, and C. Lin, "Theoretical investigation of nanowaveguide-based optical coupler using mode expansion transfer matrix," Microw. Opt. Technol. Lett. **52**(5), 1123–1129 (2010).
21. L. Tong, J. Lou, and E. Mazur, "Single-mode guiding properties of subwavelength-diameter silica and silicon wire waveguides," Opt. Express **12**(6), 1025–1035 (2004).
22. M. Sumetsky, "How thin can a microfiber be and still guide light?" Opt. Lett. **31**(7), 870–872 (2006).
23. Y. Jung, G. Brambilla, and D. J. Richardson, "Broadband single-mode operation of standard optical fibers by using a sub-wavelength optical wire filter," Opt. Express **16**(19), 14661–14667 (2008).

1. Introduction

Micro/nano fibers (MNFs) have attracted considerable interests in recent years [1, 2], as they exhibit a number of exciting properties such as large evanescent field, strong confinement, easy configurability and high robustness. The emergence of MNFs provides opportunities for the construction of versatile MNF-based photonic devices for applications in high-sensitive optical sensors [3–5], nonlinear optics [6–9], atom trapping [10], micro/nano-scale photonic devices [11–18]. MNFs can be evanescently coupled to form various micro/nano-scale photonic devices, of which the evanescent coupling between MNFs plays an important role and determines the performances of the micro/nano-scale photonic devices. It is thus essential to study both theoretically and experimentally the coupling performances between MNFs. Ref [19]. presents a model for the evanescent coupling between two parallel nanowires and Ref [20]. shows more detailed theoretical analysis for nanowaveguide-based optical couplers. However, in these works, micro/nano waveguides are all assumed to have uniform diameters, neglecting the diameter longitudinal variation. Usually, the MNFs dawn form single-mode fibers are not perfectly uniform and prone to be conical (the fiber diameter changes according to an exponential function [14]), which as a result leads to distinct coupling performances.

In this paper, we investigate the evanescent coupling characteristics between two conical micro/nano fibers by simulation and experiment. First, the evanescent coupling between two conical micro/nano fibers (CMNFs) is numerically studied using finite element method (FEM) and its performance is compared with that of uniform MNFs (UMNFs). Second, the dependence of coupling performances on the longitudinal profile of the CMNFs (semi-angle of the CMNF cones) is studied in detail. Next, a CMNF-based coupler is experimentally demonstrated and characterized. High coupling efficiency of >90% is achieved. The "box-shape" spectral response of the coupler is observed, indicating it can potentially be used as a filter. Experimental results also show that the coupling efficiency between two CMNFs is overlapping length and taper angle dependent. Finally, conclusions are given.

2. Numerical simulations

Coupled mode theory is routinely employed for weekly coupled single mode fibers. However, in the case of coupling between CMNFs where the fiber diameter is reduced to the wavelength scale, the evanescent field becomes very strong and the errors associated with the coupled mode theory are no longer negligible [20, 21]. To accurately model the coupling behavior, rigorous methods can be used by directly solving Maxwell's equations. Nonetheless, they are always complex and take considerable computer resources to solve the equations. In this consideration, here we use FEM to numerically study the coupling behaviors between CMNFs by some commercial software, e.g. COMSOL Multiphysics, ANSYS, etc. The Finite Element Method is a good choice for solving partial differential equations (PDE) over complicated domains. Its basic principle is that meshing a continuous domain into a set of discrete sub-domain, usually called elements.

In general, there three steps for numerically solving PDE using FEM: pre-processing, solving problem, and post-processing. All of these steps can be finished by the FEM

#138036 - $15.00 USD Received 11 Nov 2010; revised 9 Dec 2010; accepted 4 Jan 2011; published 14 Feb 2011

simulation software. Figure 1 shows the CMNF-based coupler model established by this software. Inset II in Fig. 1 is a three-dimensional drawing of the coupler. The CMNF pairs are assumed to have an identical shape. *D1* and *D2* are the top and bottom diameters of CMNF cone and $D(z)$ is the diameter along the fiber length, which varies with the longitudinal axis z. α is the tapering angle of the CMNF, defined as the half-angle of the CMNF core as shown in Inset I. When $\alpha = 0$, the CMNF becomes a UMNF. S is the separation distance between the CMNFs. We assume the two CMNFs are in close contact with each other, *i.e.*, $S = 0$, which is always the case due to the strong van der Waals and electrostatic forces between them. H and L are the height and overlapping length of the CMNFs.

The V number can be expressed as $V(z) = 2\pi[D(z)/2\lambda_0](n_1^2-n_2^2)^{1/2}$, where n_1 (≈1.45) and n_2 (≈1) are the refractive indices of the CMNFs and air, λ_0 is the optical wavelength in free space, here we set the wavelength λ_0 at 1550 nm. To maintain a single-mode, the V number and thus the fiber diameter $D(z)$ should be small. On the other hand, $D(z)$ should not be too small so that light can be still confined in the CMNF [22]. Thus, in the simulations and experiments below, we choose $D1 < 1200$ nm, $D2 > 300$ nm, and $\alpha < 0.12°$. In simulation, the light is input from cone1 and collected from cone2. The coupling efficiency (η) is defined as: $\eta = P_{output}/P_{input}$, where P_{input} and P_{output} are the light power at the input port and output port, respectively.

We use an ideal model as shown in Fig. 1 to perform our simulation. In practical situation, for achieve the best coupling efficiency, the optimal parameters of CMNF, for example diameter, half-angle, and overlapping length, is necessary. However, in this paper, we only place the emphasis on analyzing the influence of the overlapping length and taper angle on coupling characteristics. In order to reduce the complexity of problem, a simplified ideal model without optimizing the parameters of CMNF is adopted, which is helpful for us to focus what we concern.

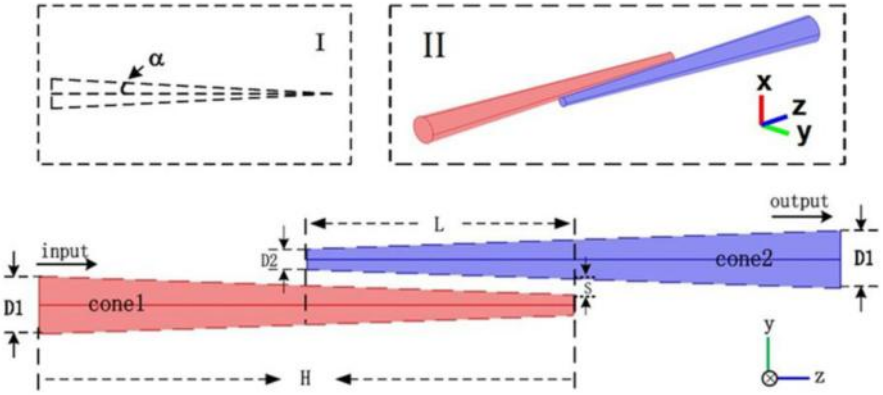

Fig. 1. Coupling structure between two CMNFs. Inset I shows the definition of the fiber cone half-angle α; Inset II shows the perspective view of coupler.

We first investigate the effect of overlapping length on coupling performances. Figure 2 shows the optical power distribution along z direction in cone2 (assuming input is from cone1). Figures 2(b)-2(d) show the optical power distribution for couplers formed by CMNFs with various overlapping lengths of L = 40 μm, 80 μm, 140 μm, respectively. H, *D1* and α remain constant at H = 160μm, *D1* = 1120 nm and $\alpha = 0.0917°$. The output power is normalized to the input power. As a comparison, the optical power distribution for the UMNF-based coupler with a diameter of 1120 nm (equal to *D1*) is also calculated (shown in Fig. 2(a)). The coupled power for the UMNF-based coupler is a periodic function of z, similar to the previous results [19]. The coupled optical power for CMNF-based coupler is also z dependent. However, distinct from the UMNF case, the power exchange between two CMNFs is not a rigorous periodic function. When the overlapping lengths between the two CMNFs in Figs. 2(b) and 2(c) are 40 and 80 μm, the periodic oscillation of coupled power also occurs, similar to the uniform MNFs case, but the average coupled power in cone2

#138036 - $15.00 USD Received 11 Nov 2010; revised 9 Dec 2010; accepted 4 Jan 2011; published 14 Feb 2011

increases along the *z* direction. When the overlapping length increases to 140 μm (Fig. 2(d)), the coupled power gradually converges to a stable value of ~0.92. In other words, there is no obvious power circulation between these two CMNFs. It can be explained by the mode coupling theory. Assuming the propagation constants in cone1 and cone2 are $\beta_1(z)$ and $\beta_2(z)$ respectively. We define the difference in propagation constant between them as $\Delta\beta$ $(=\beta_1(z)-\beta_2(z))$. Thus, in overlapping region, from left to right, the $\Delta\beta$ is changed from positive to zero and then to negative. In this processing, the power distribution between two CMNFs is determined by the value of $\Delta\beta$ and the radiuses of CMNFs. As we know the optical energy tries to stay in the CMNF with high effective refractive index. So, in the leftmost position of overlapping region, the optical energy in cone1 is dominant as shown in Fig. 2 (b)-(d). However, if the $\Delta\beta$ is not large enough, the optical energy will oscillate obviously between two CMNFs as shown in Fig. 2(b)-(c). Around the central part of overlapping region, the $\Delta\beta$ is changed from the positive to negative. In other words, the propagation constant in cone2 is gradually dominant, and as a result, the optical energy in cone1 is gradually transferred to cone2. We can see from Fig. 1 if the overlapping length is longer, the radiuses of CMNFs in the center of overlapping region will be larger, and as a result the coupling coefficient will be smaller, so the transfer length will be longer. Therefore, there is a longer slope in Fig. 2 (d) than Fig. 2 (c). Thus, due to the conical shape of the CMNF, its coupling characteristics are distinct from those of UMNF-based couplers, and as long as the coupling length is long enough, optical power can always transfer from one CMNF to the other with low coupling loss.

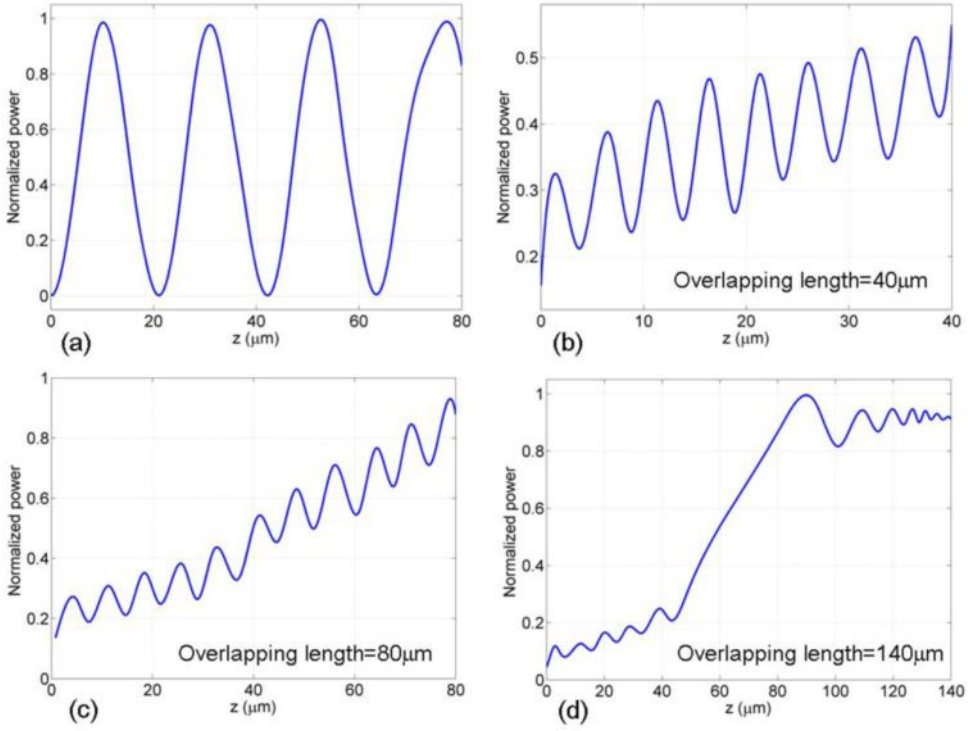

Fig. 2. Optical power distribution along *z* direction in cone2 (assume optical is input from cone1). The output power is normalized by input power. (a) is the uniform MNFs coupling case; (b)-(d) are the CMNFs coupling with overlapping length 40, 80, and 140 μm.

Figure 3 (Media1) intuitively illustrates the optical power flow in the MNF-based couplers. Figure 3(a) shows the optical power flow pattern for the coupler formed by UMNFs with a diameter of 1120 nm. Light circulates between these two UMNFs, resulting in a strong oscillation pattern. Figures 3(b) and 3(c) show the optical power flow for couplers formed by

#138036 - $15.00 USD Received 11 Nov 2010; revised 9 Dec 2010; accepted 4 Jan 2011; published 14 Feb 2011

CMNFs with coupling lengths of L = 80 μm, 140 μm, respectively. In these cases, optical power oscillation is less obvious, and the energy exchange is even smaller approaching the coupler end. There is almost not energy exchange when L = 140μm as shown in Fig. 3(c) (Media 1). It can be seen that light travels in a zigzag path when the coupler is formed by UMNFs (Fig. 3 (a) (Media 1)) or when the overlapping length is short (Fig. 3 (b) (Media 1)), and yet when the overlapping is relatively long, light travels almost in a straight line (Fig. 3 (c) (Media 1)).

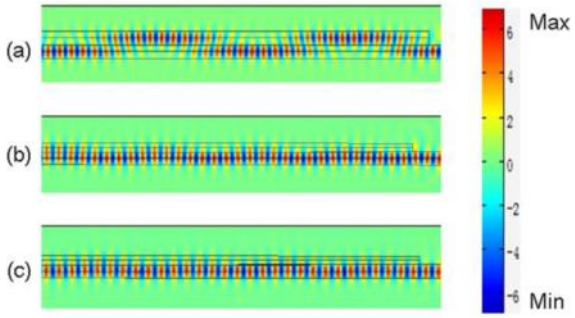

Fig. 3. Optical power flow pattern (Media 1) between (a) two sub-wavelength fibers with uniform diameters and (b)-(c) two CMNFs with overlapping lengths of (b) 80μm (c) 140μm. For clarity, only the right end parts of the couplers are shown.

The longitudinal profile of the CMNF determines the distribution of its evanescent field along the CMNF, and eventually affects the coupling characteristics of the CMNF-based coupler. The coupling performances not only depend on the overlapping length but also the CMNF diameter variation rate or its tapering angle α. Figure 4 shows the coupling efficiency varies with overlapping length for α = 0.057°, 0.0458°, and 0.1146°, respectively. With the increase of overlapping length, the coupling efficiency oscillation weakens which is more obvious for larger α's. When α ≤ 0.0458°, the coupling oscillation damping is not significant. Especially, when α = 0.0057°, its coupling behavior is almost identical to that of UMNFs. In contrast, when α is relatively large (*e.g.*, α = 0.1146°), the coupling oscillation damps very rapidly and the coupling efficiency gradually converges to a stable value. Hence, it implies that CMNFs with a large tapering angle can be used to ensure a fast convergence of the coupling efficiency and thus more compact couplers can be implemented.

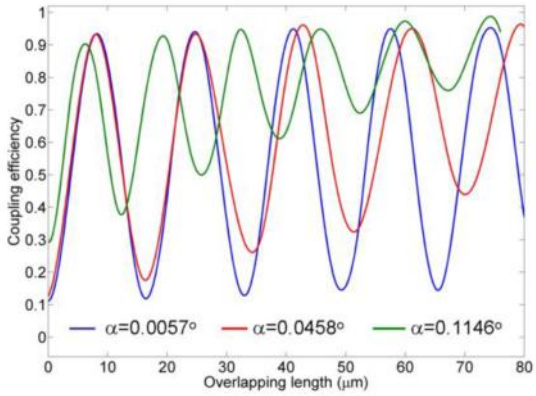

Fig. 4. Coupling efficiency versus overlapping length for three CMNF tapering angles.

#138036 - $15.00 USD Received 11 Nov 2010; revised 9 Dec 2010; accepted 4 Jan 2011; published 14 Feb 2011

3. Experiments

3.1 Fabrication of CMNFs-based couplers

The CMNFs are drawn from standard single-mode fibers using a hydrogen flame-heated technique. The conical tapering of the MNFs is realized by reliable control of the hot zone and precise movement of stage to which the fibers are attached. The waist diameter of a typical MNF is 1-2μm and the MNF length including two symmetric tapering regions is about 46 mm. We cleave each MNF into two in the middle (near the minimum waist position) to get a pair of CMNFs with a nearly identical tapering profile and use them to perform the evanescent coupling experiments.

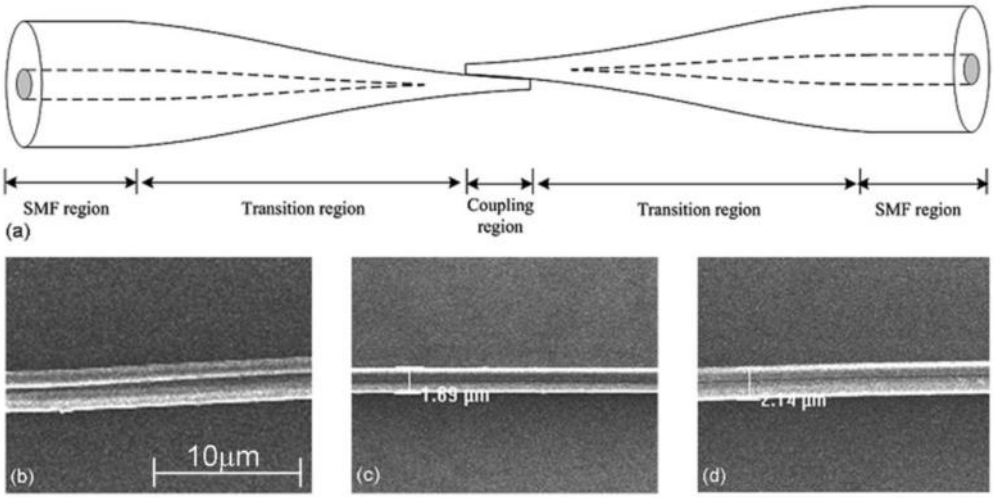

Fig. 5. (a) Schematic diagram of the conical MNF-based coupler. (b)-(c) SEM images of the attached MNFs and MNFs with two different waist diameters of 1.69μm and 2.14μm, respectively. SMF: single mode fiber.

When two CMNFs are brought in close proximity in air, they attract each other through Van der Waals or electrostatic forces, resulting in tight contact. A self-aligned evanescent coupler is thus formed. Figure 5(a) shows the schematic structure of the CMNF-based coupler used in the experiments. Figure 5(b) shows the scanning electron microscope (SEM) image of the coupling region and Fig. 5(c) and (d) show the SEM images of two single CMNFs with minimum diameters of 1.69μm and 2.14μm, respectively.

3.2 Optical characterization of CMNF-based couplers

Due to the tight attractive force between the two CMNFs, in the experiment we let the CMNFs-based coupler floating in the air and fix the pigtails on high precision optical stage with an accuracy of 10 μm. To vary the overlapping length, we simply pull one CMNF by the high precision optical stage while the other remains in contact.

First, the output spectrum of the coupler is observed. An optical source (Agilent 83438A ERBIUM ASE SOURE) is used to couple light into one port of the CMNF-based coupler, and the output spectrum is measured by an optical spectrum analyzer (ANRITSU MS9710B) from the other port. Figure 6 shows the measured spectrums for the CMNF-based coupler with a waist diameter (*D2*) of 1.69μm and an overlapping length of 75μm (blue line) and 50μm (red line) respectively. "Box-shape" spectral profiles resembling flat-top bandpass filters are observed. The insert shows the close-up view in the 1550-1554 nm spectral range. The "box-shape" spectral profile has a relatively flat top and a fast roll-off with its 3-dB bandwidth of 2 nm (although its extinction ratio is only 3-5 dB).The filter spectrum can be explained by mode coupling. As we know, the profile of CMNF determines what kinds of optical modes that be guided by this CMNF. The criterion for adiabatic propagation can be expressed as Ω =

#138036 - $15.00 USD Received 11 Nov 2010; revised 9 Dec 2010; accepted 4 Jan 2011; published 14 Feb 2011

$r(z)(\beta_1-\beta_2)/2\pi$ [23], where β_1 (lower-order mode) and β_2 (higher-order mode) are the propagation constants of two optical modes, $r(z)$ is the radius of CMNF, and Ω is the critical angle. If $\alpha<\Omega$, the CMNF is adiabatic for lower-order mode, otherwise, it is non-adiabatic. Under non-adiabatic propagation, the lower-order optical mode will excite higher-order optical modes. From the adiabatic criterion, the profile of CMNF, including radius, length and half-angle, determines which higher-order optical mode can be excited. Then the modes (lower-order, higher-order) coherently interfere and beat with each other in the overlapping region, resulting in the optical power oscillating between the two CMNFs. The oscillatory spectrum can then be observed in the output port. If the half-angle α is very large, more higher-order optical modes will be exited and then the "box-shape" output spectrum will be observed. Therefore, we can control the filter spectrum by optimizing the half-angle, radius and length of CMNF. In addition, as presented in section 2, coupling efficiency is overlapping length dependent, so the output spectrum can be easily controlled by changing the overlapping length. As shown in Fig. 6, the output spectrum is shifted while the overlapping length is changed. It implies this architecture can be potentially used as a filter by carefully controlling the profiles and overlapping length of CMNFs, which provides an alternative way for designing micro/nano-scale filters.

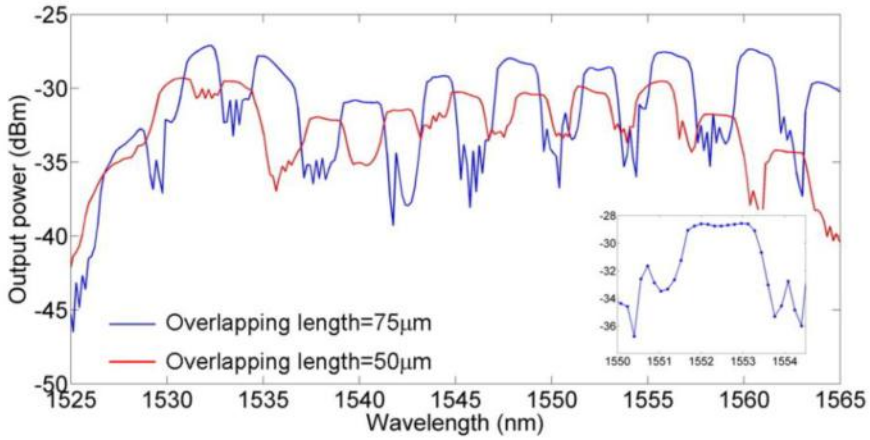

Fig. 6. Measured spectral response of a CMNFs-based coupler with different overlapping length. Inset shows the close-up view of one transmission peak.

Figure 7(a) shows the measured coupling efficiency as a function of CMNF overlapping length L for the CMNFs with a 2.14 μm waist diameter at 1550 nm. The coupling efficiency exhibits periodic oscillation with the overlapping length due to mode beating as in a direction coupler [19]. However, distinct from the couplers composed by uniform fibers or waveguides [19], here the oscillation magnitude decreases and oscillation period increases with the overlapping length, which is more obvious when a long overlapping length is examined. Figure 7(b) shows the measured coupling efficiency for the pair of CMNFs with a waist diameter of about 1.69μm. Similar to the previous case, the coupling efficiency experiences a damped oscillation when overlapping length increases. When the overlapping length reaches about 1mm, the coupling efficiency gradually stabilizes at > 90%, indicating that beyond a certain overlapping length, almost all the energy can be transferred from one CMNF to the other without circulating back. It thus implies that as long as the overlapping length is long enough (exceeding the damping length), we can always get a stable high coupling efficiency using our CMNF-based couplers, therefore easing coupler design and alleviating the troublesome in accurate alignment. The experimental observations also show the overlapping length and taper angle dependence, which verified the conclusions drawn from the simulation.

#138036 - $15.00 USD Received 11 Nov 2010; revised 9 Dec 2010; accepted 4 Jan 2011; published 14 Feb 2011

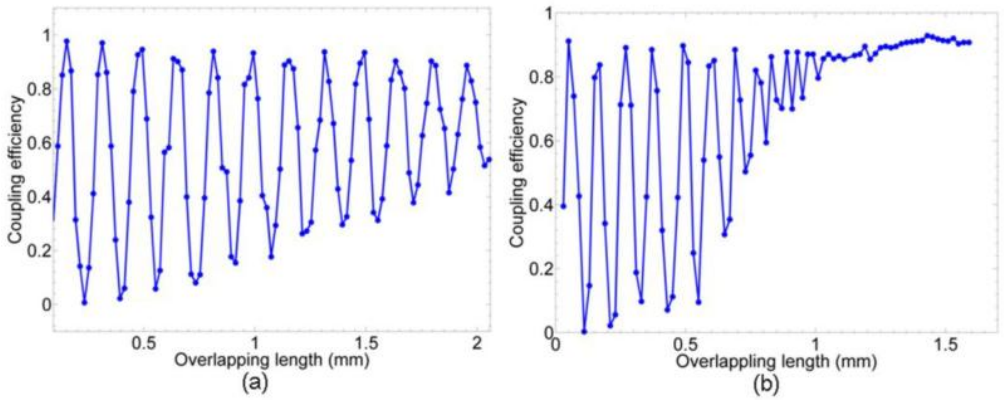

Fig. 7. Measured coupling efficiency versus overlapping length for the CMNF-based couplers. The diameters of CMNFs for (a) and (b) are 2.14 μm and 1.69 μm, respectively. Both (a) and (b) experience a damped oscillation when overlapping length increases, and yet damping length for (a) is longer than (b).

4. Conclusions

In summary, we investigated the evanescent coupling between two CMNFs by simulation and experiment. Compared to the coupler formed by UMNFs, the CMNF-based coupler exhibits unique transmission characteristics. Optical power is gradually coupled from one CMNF to the other in a damped oscillation and the coupling efficiency gradually converges with the increase of the overlapping length. The convergence is more rapid for larger CMNF tapering angles. We also experimentally demonstrated the CMNF-based couplers. A stable coupling efficiency of >90% is obtained. The transmission spectrum of the CMNF-based coupler shows a high-order filtering performance as a result of the coherent interference among optical modes in the CMNFs. We believe our work is of significance for micro/nano-fiber-based photonic devices design. It provides a method for efficient light coupling between two micro/nano-fibers and can find a variety of applications in on-chip optical interconnect and optical signal processing.

Acknowledgments

This work was supported in part by 973 program (ID2011CB301700), NSFC (60877012, 61071011, 61001074, 61007039, 61007052), MOE New Faculty Foundation (200802481012), STCSM Project (10DJ1400402, 09JC1408100), SMEC Innovation Program (09ZZ185), Hangtian Research Institute-SJTU Joint Foundation, State Key Lab Projects (GKZD030004/09/15/20/21), Project of MOE Key Lab of Optical Fiber Sensing & Communications (UESTC), Shanghai Jiao Tong University Innovation Fund For Postgraduates.

#138036 - $15.00 USD Received 11 Nov 2010; revised 9 Dec 2010; accepted 4 Jan 2011; published 14 Feb 2011